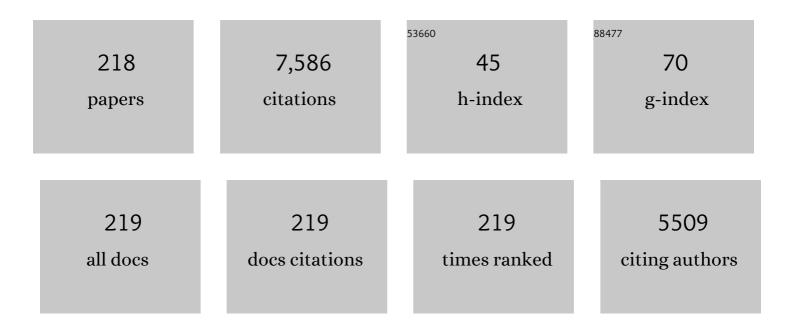
## Li-Long Jiang

List of Publications by Year in descending order

Source: https://exaly.com/author-pdf/2433133/publications.pdf Version: 2024-02-01



#	Article	IF	CITATIONS
1	Geometrical-Site-Dependent Catalytic Activity of Ordered Mesoporous Co-Based Spinel for Benzene Oxidation: In Situ DRIFTS Study Coupled with Raman and XAFS Spectroscopy. ACS Catalysis, 2017, 7, 1626-1636.	5.5	281
2	Insight into the effect of morphology on catalytic performance of porous CeO2 nanocrystals for H2S selective oxidation. Applied Catalysis B: Environmental, 2019, 252, 98-110.	10.8	213
3	Activity and Stability Boosting of an Oxygenâ€Vacancyâ€Rich BiVO <sub>4</sub> Photoanode by NiFeâ€MOFs Thin Layer for Water Oxidation. Angewandte Chemie - International Edition, 2021, 60, 1433-1440.	7.2	205
4	Insights into the high performance of Mn-Co oxides derived from metal-organic frameworks for total toluene oxidation. Journal of Hazardous Materials, 2018, 349, 119-127.	6.5	191
5	Effect of alloy composition on catalytic performance and coke-resistance property of Ni-Cu/Mg(Al)O catalysts for dry reforming of methane. Applied Catalysis B: Environmental, 2018, 239, 324-333.	10.8	152
6	Thermodynamic and molecular insights into the absorption of H <sub>2</sub> S, CO <sub>2</sub> , and CH <sub>4</sub> in choline chloride plus urea mixtures. AICHE Journal, 2019, 65, e16574.	1.8	139
7	Enhanced catalytic activity over MIL-100(Fe) with coordinatively unsaturated Fe2+/Fe3+ sites for selective oxidation of H2S to sulfur. Chemical Engineering Journal, 2019, 374, 793-801.	6.6	114
8	Amino-Modified Fe-Terephthalate Metal–Organic Framework as an Efficient Catalyst for the Selective Oxidation of H <sub>2</sub> S. Inorganic Chemistry, 2018, 57, 10081-10089.	1.9	106
9	Morphology Effect of Ceria on the Catalytic Performances of Ru/CeO <sub>2</sub> Catalysts for Ammonia Synthesis. Industrial & Engineering Chemistry Research, 2018, 57, 9127-9135.	1.8	105
10	Polymeric carbon nitride nanomesh as an efficient and durable metal-free catalyst for oxidative desulfurization. Chemical Communications, 2018, 54, 2475-2478.	2.2	104
11	Promoted adsorption of CO <sub>2</sub> on amineâ€impregnated adsorbents by functionalized ionic liquids. AICHE Journal, 2018, 64, 3671-3680.	1.8	98
12	Ammonia Synthesis Activity of Alumina-Supported Ruthenium Catalyst Enhanced by Alumina Phase Transformation. ACS Catalysis, 2019, 9, 1635-1644.	5.5	96
13	Ru-Based Catalysts for Ammonia Decomposition: A Mini-Review. Energy & amp; Fuels, 2021, 35, 11693-11706.	2.5	89
14	Isolated iron sites embedded in graphitic carbon nitride (g-C3N4) for efficient oxidative desulfurization. Applied Catalysis B: Environmental, 2020, 267, 118663.	10.8	86
15	Designing Low-Viscosity Deep Eutectic Solvents with Multiple Weak-Acidic Groups for Ammonia Separation. ACS Sustainable Chemistry and Engineering, 2021, 9, 7352-7360.	3.2	86
16	Carbon dioxide reforming of methane over Ni catalysts prepared from Ni–Mg–Al layered double hydroxides: Influence of Ni loadings. Fuel, 2015, 162, 271-280.	3.4	84
17	Nitrogen-Decorated, Ordered Mesoporous Carbon Spheres as High-Efficient Catalysts for Selective Capture and Oxidation of H <sub>2</sub> S. ACS Sustainable Chemistry and Engineering, 2019, 7, 7609-7618.	3.2	84
18	Exfoliation of Graphitic Carbon Nitride for Enhanced Oxidative Desulfurization: A Facile and General Strategy. ACS Sustainable Chemistry and Engineering, 2019, 7, 4941-4950.	3.2	82

#	Article	IF	CITATIONS
19	Catalytic Activity and Stability over Nanorod-Like Ordered Mesoporous Phosphorus-Doped Alumina Supported Palladium Catalysts for Methane Combustion. ACS Catalysis, 2018, 8, 11016-11028.	5.5	78
20	Highly Efficient Porous Fe <i><sub>x</sub></i> Ce <sub>1–<i>x</i></sub> O <sub>2â^'Î</sub> with Three-Dimensional Hierarchical Nanoflower Morphology for H <sub>2</sub> S-Selective Oxidation. ACS Catalysis, 2020, 10, 3968-3983.	5.5	78
21	Construction of Fe-doped TiO2â^'x ultrathin nanosheets with rich oxygen vacancies for highly efficient oxidation of H2S. Chemical Engineering Journal, 2022, 430, 132917.	6.6	77
22	Low temperature desulfurization on Co-doped α-FeOOH: Tailoring the phase composition and creating the defects. Chemical Engineering Journal, 2016, 306, 124-130.	6.6	74
23	Hierarchically porous γ-Al2O3 nanosheets: Facile template-free preparation and reaction mechanism for H2S selective oxidation. Chemical Engineering Journal, 2018, 346, 238-248.	6.6	74
24	Fe-doped γ-Al <sub>2</sub> O <sub>3</sub> porous hollow microspheres for enhanced oxidative desulfurization: facile fabrication and reaction mechanism. Green Chemistry, 2018, 20, 4645-4654.	4.6	74
25	MnO2 nanoparticles encapsuled in spheres of Ce-Mn solid solution: Efficient catalyst and good water tolerance for low-temperature toluene oxidation. Applied Surface Science, 2020, 504, 144481.	3.1	73
26	Insight into dynamic and steady-state active sites for nitrogen activation to ammonia by cobalt-based catalyst. Nature Communications, 2020, 11, 653.	5.8	72
27	Effects of anaerobic SO2 treatment on nano-CeO2 of different morphologies for selective catalytic reduction of NOx with NH3. Chemical Engineering Journal, 2020, 382, 122910.	6.6	68
28	Challenges and Opportunities of Ru-Based Catalysts toward the Synthesis and Utilization of Ammonia. ACS Catalysis, 2022, 12, 3938-3954.	5.5	67
29	Structure–Activity Relationships of AMn <sub>2</sub> O <sub>4</sub> (A = Cu and Co) Spinels in Selective Catalytic Reduction of NO <sub><i>x</i></sub> : Experimental and Theoretical Study. Journal of Physical Chemistry C, 2017, 121, 3339-3349.	1.5	62
30	Design of Efficient, Hierarchical Porous Polymers Endowed with Tunable Structural Base Sites for Direct Catalytic Elimination of COS and H <sub>2</sub> S. ACS Applied Materials & Interfaces, 2019, 11, 29950-29959.	4.0	61
31	Enhanced Ammonia Synthesis Activity of Ceria-Supported Ruthenium Catalysts Induced by CO Activation. ACS Catalysis, 2021, 11, 1331-1339.	5.5	61
32	Effect of ceria morphology on the catalytic activity of Co/CeO2 catalyst for ammonia synthesis. Catalysis Communications, 2017, 101, 15-19.	1.6	60
33	Promoting effect of Cu-doping on catalytic activity and SO2 resistance of porous CeO2 nanorods for H2S selective oxidation. Journal of Catalysis, 2020, 389, 382-399.	3.1	59
34	Size sensitivity of supported Ru catalysts for ammonia synthesis: From nanoparticles to subnanometric clusters and atomic clusters. CheM, 2022, 8, 749-768.	5.8	59
35	Total oxidation of benzene over ACo 2 O 4 (A = Cu, Ni and Mn) catalysts: In situ DRIFTS account for understanding the reaction mechanism. Applied Surface Science, 2017, 426, 1198-1205.	3.1	58
36	Synthesis of Co–Mn oxides with double-shelled nanocages for low-temperature toluene combustion. Catalysis Science and Technology, 2018, 8, 4494-4502.	2.1	58

#	Article	IF	CITATIONS
37	Structural requirements of manganese oxides for methane oxidation: XAS spectroscopy and transition-state studies. Applied Catalysis B: Environmental, 2018, 229, 52-62.	10.8	57
38	Efficient catalytic elimination of COS and H2S by developing ordered mesoporous carbons with versatile base N sites via a calcination induced self-assembly route. Chemical Engineering Science, 2020, 221, 115714.	1.9	55
39	Highly efficient and selective separation of ammonia by deep eutectic solvents through cooperative acid-base and strong hydrogen-bond interaction. Journal of Molecular Liquids, 2021, 337, 116463.	2.3	55
40	Ni/Al2O3-ZrO2 catalyst for CO2 methanation: The role of γ-(Al, Zr)2O3 formation. Applied Surface Science, 2018, 459, 74-79.	3.1	52
41	MOF-derived porous Fe <sub>2</sub> O <sub>3</sub> with controllable shapes and improved catalytic activities in H <sub>2</sub> S selective oxidation. CrystEngComm, 2018, 20, 3449-3454.	1.3	51
42	Porous nanosheets of carbon-conjugated graphitic carbon nitride for the oxidation of H2S to elemental sulfur. Carbon, 2019, 155, 204-214.	5.4	51
43	Selective catalytic tailoring of the H unit in herbaceous lignin for methyl <i>p</i> -hydroxycinnamate production over metal-based ionic liquids. Green Chemistry, 2018, 20, 3743-3752.	4.6	50
44	Spatial Confinement of Electron-Rich Ni Nanoparticles for Efficient Ammonia Decomposition to Hydrogen Production. ACS Catalysis, 2021, 11, 10345-10350.	5.5	49
45	Atomically Dispersed Ru Catalyst for Low-Temperature Nitrogen Activation to Ammonia via an Associative Mechanism. ACS Catalysis, 2020, 10, 9504-9514.	5.5	47
46	Interfacial Engineering Promoting Electrosynthesis of Ammonia over Mo/Phosphotungstic Acid with High Performance. Advanced Functional Materials, 2021, 31, 2009151.	7.8	47
47	Engineering of crystal phase over porous MnO2 with 3D morphology for highly efficient elimination of Hazardous Materials, 2021, 411, 125180.	6.5	47
48	Layered double hydroxides as precursors of Cu catalysts for hydrogen production by water-gas shift reaction. International Journal of Hydrogen Energy, 2015, 40, 10016-10025.	3.8	46
49	Cu/CeO <sub>2</sub> Catalyst for Waterâ€Gas Shift Reaction: Effect of CeO <sub>2</sub> Pretreatment. ChemPhysChem, 2018, 19, 1448-1455.	1.0	46
50	Techno-economic analysis and comprehensive optimization of an <i>on-site</i> hydrogen refuelling station system using ammonia: hybrid hydrogen purification with both high H <sub>2</sub> purity and high recovery. Sustainable Energy and Fuels, 2020, 4, 3006-3017.	2.5	46
51	Construction of cross-linked δ-MnO2 with ultrathin structure for the oxidation of H2S: Structure-activity relationship and kinetics study. Applied Catalysis B: Environmental, 2021, 297, 120402.	10.8	46
52	llluminate the active sites of $\hat{I}^3$ -FeOOH for low-temperature desulfurization. Applied Surface Science, 2017, 425, 212-219.	3.1	44
53	Low-Temperature H <sub>2</sub> S Removal from Gas Streams over γ-FeOOH, γ-Fe <sub>2</sub> O <sub>3</sub> , and α-Fe <sub>2</sub> O <sub>3</sub> : Effects of the Hydroxyl Group, Defect, and Specific Surface Area. Industrial & Engineering Chemistry Research, 2019, 58, 19353-19360.	1.8	44
54	<scp>Chelationâ€activated multipleâ€site</scp> reversible chemical absorption of ammonia in ionic liquids. AICHE Journal, 2022, 68, .	1.8	44

#	Article	IF	CITATIONS
55	Rational designed Co@N-doped carbon catalyst for high-efficient H2S selective oxidation by regulating electronic structures. Chemical Engineering Journal, 2020, 401, 126038.	6.6	43
56	Cobalt-aluminum mixed oxides prepared from layered double hydroxides for the total oxidation of benzene. Applied Catalysis A: General, 2015, 507, 130-138.	2.2	42
57	Synthesis of Mg-Doped Ordered Mesoporous Pd–Al <sub>2</sub> O <sub>3</sub> with Different Basicity for CO, NO, and HC Elimination. Industrial & Engineering Chemistry Research, 2017, 56, 1687-1695.	1.8	41
58	Mechanochemically synthesized MgAl layered double hydroxide nanosheets for efficient catalytic removal of carbonyl sulfide and H <sub>2</sub> S. Chemical Communications, 2019, 55, 9375-9378.	2.2	41
59	Highly Active and Sulfurâ€Resistant Fe–N <sub>4</sub> Sites in Porous Carbon Nitride for the Oxidation of H <sub>2</sub> S into Elemental Sulfur. Small, 2020, 16, e2003904.	5.2	41
60	Hydrotalcite-derived Co/Mg(Al)O as a stable and coke-resistant catalyst for low-temperature carbon dioxide reforming of methane. Applied Catalysis A: General, 2018, 552, 21-29.	2.2	40
61	Influence of Ru Substitution on the Properties of LaCoO <sub>3</sub> Catalysts for Ammonia Synthesis: XAFS and XPS Studies. Industrial & Engineering Chemistry Research, 2018, 57, 17375-17383.	1.8	40
62	Enhanced ammonia synthesis performance of ceria-supported Ru catalysts <i>via</i> introduction of titanium. Chemical Communications, 2020, 56, 1141-1144.	2.2	40
63	Enhanced Selective H <sub>2</sub> S Oxidation Performance on Mo <sub>2</sub> C-Modified g-C <sub>3</sub> N <sub>4</sub> . ACS Sustainable Chemistry and Engineering, 2019, 7, 16257-16263.	3.2	39
64	Synthesis and application of highly dispersed ordered mesoporous silicon-doped Pd-alumina catalyst with high thermal stability. Chemical Engineering Journal, 2016, 297, 148-157.	6.6	38
65	A solvent-free, one-step synthesis of sulfonic acid group-functionalized mesoporous organosilica with ultra-high acid concentrations and excellent catalytic activities. Green Chemistry, 2018, 20, 1020-1030.	4.6	38
66	Deactivation study of carbon-supported ruthenium catalyst with potassium promoter. Applied Catalysis A: General, 2017, 541, 1-7.	2.2	37
67	Facile fabrication of shape-controlled Co <sub>x</sub> Mn <sub>y</sub> O <sub>β</sub> nanocatalysts for benzene oxidation at low temperatures. Chemical Communications, 2018, 54, 2154-2157.	2.2	37
68	Coupling ammonia catalytic decomposition and electrochemical oxidation for solid oxide fuel cells: A model based on elementary reaction kinetics. Journal of Power Sources, 2019, 423, 125-136.	4.0	37
69	Characterization and Catalytic Performance of Cu/ZnO/Al <sub>2</sub> O <sub>3</sub> Water–Gas Shift Catalysts Derived from Cu–Zn–Al Layered Double Hydroxides. Industrial & Engineering Chemistry Research, 2017, 56, 3175-3183.	1.8	36
70	Strong metal–support interactions of Co-based catalysts facilitated by dopamine for highly efficient ammonia synthesis: <i>in situ</i> XPS and XAFS spectroscopy coupled with TPD studies. Chemical Communications, 2019, 55, 474-477.	2.2	36
71	Morphology evolution of acetic acid-modulated MIL-53(Fe) for efficient selective oxidation of H2S. Chinese Journal of Catalysis, 2021, 42, 279-287.	6.9	36
72	Improving the ammonia synthesis activity of Ru/CeO2 through enhancement of the metal–support interaction. Journal of Energy Chemistry, 2021, 60, 403-409.	7.1	36

#	Article	IF	CITATIONS
73	Geometric structure distribution and oxidation state demand of cations in spinel NixFe1-xCo2O4 composite cathodes for solid oxide fuel cells. Chemical Engineering Journal, 2021, 425, 131822.	6.6	36
74	Facile Strategy to Extend Stability of Simple Component-Alumina-Supported Palladium Catalysts for Efficient Methane Combustion. ACS Applied Materials & Interfaces, 2020, 12, 56095-56107.	4.0	36
75	An Ammonia–Hydrogen Energy Roadmap for Carbon Neutrality: Opportunity and Challenges in China. Engineering, 2021, 7, 1688-1691.	3.2	36
76	Operando spectroscopic and isotopic-label-directed observation of LaN-promoted Ru/ZrH2 catalyst for ammonia synthesis via associative and chemical looping route. Journal of Catalysis, 2020, 389, 218-228.	3.1	35
77	Highly efficient ammonia synthesis at low temperature over a Ru–Co catalyst with dual atomically dispersed active centers. Chemical Science, 2021, 12, 7125-7137.	3.7	35
78	Synthesis of a Highly Stable Pd@CeO <sub>2</sub> Catalyst for Methane Combustion with the Synergistic Effect of Urea and Citric Acid. ACS Omega, 2018, 3, 16769-16776.	1.6	34
79	Iron-Based Metal–Organic Frameworks as Platform for H <sub>2</sub> S Selective Conversion: Structure-Dependent Desulfurization Activity. Inorganic Chemistry, 2020, 59, 4483-4492.	1.9	34
80	Magnesium-aluminum mixed metal oxide supported copper nanoparticles as catalysts for water-gas shift reaction. Fuel, 2016, 184, 382-389.	3.4	33
81	Microstructural property regulation and performance in methane combustion reaction of ordered mesoporous alumina supported palladium-cobalt bimetallic catalysts. Applied Catalysis B: Environmental, 2020, 263, 118269.	10.8	33
82	Insights into the electrochemical degradation of phenolic lignin model compounds in a protic ionic liquid–water system. Green Chemistry, 2021, 23, 1665-1677.	4.6	33
83	Pyridine-Functionalized and Metallized Meso-Macroporous Polymers for Highly Selective Capture and Catalytic Conversion of CO <sub>2</sub> into Cyclic Carbonates. Industrial & Engineering Chemistry Research, 2017, 56, 15008-15016.	1.8	32
84	Carbon support surface effects in the catalytic performance of Ba-promoted Ru catalyst for ammonia synthesis. Catalysis Today, 2018, 316, 230-236.	2.2	32
85	Highly Efficient Transfer Hydrogenation of Levulinate Esters to γ-Valerolactone over Basic Zirconium Carbonate. Industrial & Engineering Chemistry Research, 2018, 57, 10126-10136.	1.8	31
86	A green and efficient hydration of alkynes catalyzed by hierarchically porous poly(ionic liquid)s solid strong acids. Applied Catalysis A: General, 2018, 564, 56-63.	2.2	31
87	Enhancing the activity of MoS2/SiO2-Al2O3 bifunctional catalysts for suspended-bed hydrocracking of heavy oils by doping with Zr atoms. Chinese Journal of Chemical Engineering, 2021, 39, 126-134.	1.7	31
88	Aqueous and Templateâ€Free Synthesis of Meso–Macroporous Polymers for Highly Selective Capture and Conversion of Carbon Dioxide. ChemSusChem, 2017, 10, 4144-4149.	3.6	30
89	Ni–Fe/Mg(Al)O alloy catalyst for carbon dioxide reforming of methane: Influence of reduction temperature and Ni–Fe alloying on coking. International Journal of Hydrogen Energy, 2020, 45, 33574-33585.	3.8	30
90	Studies on SO <sub>2</sub> Tolerance and Regeneration over Perovskite-Type LaCo <sub>1–<i>x</i></sub> Pt <sub><i>x</i></sub> O <sub>3</sub> in NO <sub><i>x</i></sub> Storage and Reduction. Journal of Physical Chemistry C, 2014, 118, 13743-13751.	1.5	29

#	Article	IF	CITATIONS
91	Effect of Ceria Precursor on the Physicochemical and Catalytic Properties of Mn–W/CeO <sub>2</sub> Nanocatalysts for NH <sub>3</sub> SCR at Low Temperature. Industrial & Engineering Chemistry Research, 2017, 56, 14980-14994.	1.8	29
92	Facile fabrication of Ce-decorated composition-tunable Ce@ZnCo <sub>2</sub> O <sub>4</sub> core–shell microspheres for enhanced catalytic propane combustion. Nanoscale, 2019, 11, 4794-4802.	2.8	29
93	Ru surface density effect on ammonia synthesis activity and hydrogen poisoning of ceria-supported Ru catalysts. Chinese Journal of Catalysis, 2021, 42, 1712-1723.	6.9	29
94	Tuning the growth of Cu-MOFs for efficient catalytic hydrolysis of carbonyl sulfide. Chinese Journal of Catalysis, 2017, 38, 1373-1381.	6.9	28
95	Construction of Spatial Effect from Atomically Dispersed Co Anchoring on Subnanometer Ru Cluster for Enhanced N <sub>2</sub> -to-NH <sub>3</sub> Conversion. ACS Catalysis, 2021, 11, 4430-4440.	5.5	28
96	Rapid electrochemical synthesis of HKUST-1 on indium tin oxide. RSC Advances, 2017, 7, 9316-9320.	1.7	27
97	Role of Citric Acid in Preparing Highly Active CoMo/Al <sub>2</sub> O <sub>3</sub> Catalyst: From Aqueous Impregnation Solution to Active Site Formation. Industrial & Engineering Chemistry Research, 2017, 56, 14172-14181.	1.8	27
98	Sacrificial Adsorbate Strategy Achieved Strong Metal–Support Interaction of Stable Cu Nanocatalysts. ACS Applied Energy Materials, 2018, 1, 1408-1414.	2.5	27
99	Influence of reduction temperature on Ni particle size and catalytic performance of Ni/Mg(Al)O catalyst for CO2 reforming of CH4. International Journal of Hydrogen Energy, 2020, 45, 2794-2807.	3.8	27
100	Graphitic Carbon Nitride Functionalized with Polyethylenimine for Highly Effective Capture of Carbon Dioxide. Industrial & Engineering Chemistry Research, 2018, 57, 11031-11038.	1.8	26
101	Site-Oriented Design of High-Performance Halloysite-Supported Palladium Catalysts for Methane Combustion. Industrial & Engineering Chemistry Research, 2020, 59, 5636-5647.	1.8	26
102	Site-oriented design of spinel MgxNiMn2-xO4-δas cathode material of intermediate-temperature direct ammonia solid oxide fuel cell. Journal of Power Sources, 2021, 503, 230020.	4.0	26
103	Biomass-Derived Hierarchically Porous Carbons Abundantly Decorated with Nitrogen Sites for Efficient CO <sub>2</sub> Catalytic Utilization. Industrial & Engineering Chemistry Research, 2019, 58, 7980-7988.	1.8	25
104	Characterization and catalytic behavior of hydrotalcite-derived Ni–Al catalysts for methane decomposition. International Journal of Hydrogen Energy, 2020, 45, 17299-17310.	3.8	25
105	Efficient catalytic removal of COS and H2S over graphitized 2D micro-meso-macroporous carbons endowed with ample nitrogen sites synthesized via mechanochemical carbonization. Green Energy and Environment, 2022, 7, 983-995.	4.7	25
106	Inducing the Metal–Support Interaction and Enhancing the Ammonia Synthesis Activity of Ceria-Supported Ruthenium Catalyst via N <sub>2</sub> H <sub>4</sub> Reduction. ACS Sustainable Chemistry and Engineering, 2021, 9, 4885-4893.	3.2	24
107	Preparation of supported Co catalysts from Co–Mg–Al layered double hydroxides for carbon dioxide reforming of methane. International Journal of Hydrogen Energy, 2017, 42, 5063-5071.	3.8	23
108	Pyrochlore Pr2Zr2-xMxO7+Î′ (M = Al, Ga, In) solid-state electrolytes: Defect-mediated oxygen hopping pathways and enhanced NO2 sensing properties. Sensors and Actuators B: Chemical, 2018, 270, 130-139.	4.0	23

#	Article	IF	CITATIONS
109	Efficient ammonia synthesis over a core–shell Ru/CeO <sub>2</sub> catalyst with a tunable CeO <sub>2</sub> size: DFT calculations and XAS spectroscopy studies. Inorganic Chemistry Frontiers, 2019, 6, 396-406.	3.0	23
110	Facile construction of ultrastable alumina anchored palladium catalysts <i>via</i> a designed one pot strategy for enhanced methane oxidation. Catalysis Science and Technology, 2020, 10, 4612-4623.	2.1	23
111	Porous α-Fe2O3/SnO2 nanoflower with enhanced sulfur selectivity and stability for H2S selective oxidation. Chinese Chemical Letters, 2021, 32, 2143-2150.	4.8	23
112	Review on catalytic roles of rare earth elements in ammonia synthesis: Development and perspective. Journal of Rare Earths, 2022, 40, 1-10.	2.5	23
113	Tunable ionic liquids as oil-soluble precursors of dispersed catalysts for suspended-bed hydrocracking of heavy residues. Fuel, 2022, 313, 122664.	3.4	23
114	Facile synthesis of Mn–Fe/CeO <sub>2</sub> nanotubes by gradient electrospinning and their excellent catalytic performance for propane and methane oxidation. Dalton Transactions, 2017, 46, 16967-16972.	1.6	22
115	Enhanced Methane Oxidation over Co <sub>3</sub> O <sub>4</sub> –In <sub>2</sub> O <sub>3</sub> - <i>x</i> Composite Oxide Nanoparticles via Controllable Substitution of Co <sup>3+</sup> /Co <sup>2+</sup> by In <sup>3+</sup> Ions. ACS Applied Nano Materials. 2020. 3. 9470-9479.	2.4	22
116	Rational design of highly H2O- and CO2-tolerant hydroxyapatite-supported Pd catalyst for low-temperature methane combustion. Chemical Engineering Journal, 2020, 396, 125225.	6.6	22
117	Effects of Using Carbon-Coated Alumina as Support for Ba-Promoted Ru Catalyst in Ammonia Synthesis. Industrial & Engineering Chemistry Research, 2019, 58, 10285-10295.	1.8	21
118	A novel solar system integrating concentrating photovoltaic thermal collectors and variable effect absorption chiller for flexible co-generation of electricity and cooling. Energy Conversion and Management, 2020, 206, 112506.	4.4	21
119	Hierarchical N-Doped Carbons Endowed with Structural Base Sites toward Highly Selective Adsorption and Catalytic Oxidation of H <sub>2</sub> S. Industrial & Engineering Chemistry Research, 2021, 60, 2101-2111.	1.8	21
120	Sacrificial Sucrose Strategy Achieved Enhancement of Ammonia Synthesis Activity over a Ceria-Supported Ru Catalyst. ACS Sustainable Chemistry and Engineering, 2021, 9, 8962-8969.	3.2	21
121	Highly Poisonâ€Resistant Singleâ€Atom Co–N <sub>4</sub> Active Sites with Superior Operational Stability over 460Âh for H <sub>2</sub> S Catalytic Oxidation. Small, 2021, 17, e2104939.	5.2	21
122	Sulfur-resistant methane combustion invoked by surface property regulation on palladium-based catalysts. Applied Surface Science, 2022, 587, 152835.	3.1	21
123	Carboxylic functionalized mesoporous polymers for fast, highly efficient, selective and reversible adsorption of ammonia. Chemical Engineering Journal, 2022, 448, 137640.	6.6	21
124	Unraveling the size-dependent effect of Ru-based catalysts on Ammonia synthesis at mild conditions. Journal of Catalysis, 2021, 404, 501-511.	3.1	20
125	Highly-integrated and Cost-efficient Ammonia-fueled fuel cell system for efficient power generation: A comprehensive system optimization and Techno-Economic analysis. Energy Conversion and Management, 2022, 251, 114917.	4.4	20
126	Nickel‒cobalt bimetallic catalysts prepared from hydrotalcite-like compounds for dry reforming of methane. International Journal of Hydrogen Energy, 2022, 47, 24358-24373.	3.8	20

#	Article	IF	CITATIONS
127	Sulfur resistant WGS catalyst for hydrogen production based on CoMo supported by Nb modified MgAl mixed oxide. International Journal of Hydrogen Energy, 2017, 42, 29935-29943.	3.8	19
128	Molecular-level understanding of reaction path optimization as a function of shape concerning the metal–support interaction effect of Co/CeO <sub>2</sub> on water-gas shift catalysis. Catalysis Science and Technology, 2019, 9, 4928-4937.	2.1	19
129	Cu/Fe3O4 catalyst for water gas shift reaction: Insight into the effect of Fe2+ and Fe3+ distribution in Fe3O4. International Journal of Hydrogen Energy, 2020, 45, 8456-8465.	3.8	19
130	Catalytic methane oxidation performance over Pd $\hat{l}^3$ -Al2O3 catalyst optimized by the synergy of phosphorus and MOx (MÂ=ÂLa, Ba and Zr). Fuel, 2021, 299, 120933.	3.4	19
131	Optimized coupling of ammonia decomposition and electrochemical oxidation in a tubular direct ammonia solid oxide fuel cell for high-efficiency power generation. Applied Energy, 2022, 307, 118158.	5.1	19
132	Trialkylmethylammonium molybdate ionic liquids as novel oil-soluble precursors of dispersed metal catalysts for slurry-phase hydrocracking of heavy oils. Chemical Engineering Science, 2022, 253, 117516.	1.9	19
133	Integrating Dissociative and Associative Routes for Efficient Ammonia Synthesis over a TiCN-Promoted Ru-Based Catalyst. ACS Catalysis, 2022, 12, 2651-2660.	5.5	18
134	Size-dependent activity of supported Ru catalysts for ammonia synthesis at mild conditions. Journal of Catalysis, 2022, 408, 98-108.	3.1	18
135	Electronic metal-support interaction enhanced ammonia decomposition efficiency of perovskite oxide supported ruthenium. Chemical Engineering Science, 2022, 257, 117719.	1.9	18
136	Pressurized tubular solid oxide H <sub>2</sub> O/CO <sub>2</sub> coelectrolysis cell for direct powerâ€toâ€methane. AICHE Journal, 2020, 66, e16896.	1.8	17
137	Activity enhancement of ceria-supported Co-Mo bimetallic catalysts by tuning reducibility and metal enrichment. Journal of Catalysis, 2022, 406, 231-240.	3.1	17
138	Oxygen vacancy defects engineering on Cu-doped Co3O4 for promoting effective COS hydrolysis. Green Energy and Environment, 2023, 8, 831-841.	4.7	17
139	Effects of Doping Rare Earth Elements (Y, La, and Ce) on Catalytic Performances of CoMo/MgAlM for Water Gas Shift Reaction. Industrial & Engineering Chemistry Research, 2018, 57, 833-844.	1.8	16
140	Pyrochlore Pr2Zr1.95In0.05O7+l̂´oxygen conductors: Defect-induced electron transport and enhanced NO2 sensing performances. Electrochimica Acta, 2019, 293, 338-347.	2.6	16
141	Gas sensing properties of amperometric NH3 sensors based on Sm2Zr2O7 solid electrolyte and SrM2O4 (M = Sm, La, Gd, Y) sensing electrodes. Sensors and Actuators B: Chemical, 2020, 303, 127220.	4.0	16
142	A Cationic Polymerization Strategy to Design Sulfonated Micro–Mesoporous Polymers as Efficient Adsorbents for Ammonia Capture and Separation. Macromolecules, 2021, 54, 7010-7020.	2.2	16
143	Solvent-free molten co-assembly of ordered mesoporous carbon for efficiently supported adsorption and separation of SO <sub>2</sub> . Journal of Materials Chemistry A, 2022, 10, 8817-8825.	5.2	16
144	CoMo sulfur-tolerant water-gas shift catalyst derived from an Anderson-type heteropolyanion precursor. Catalysis Communications, 2016, 86, 19-22.	1.6	15

#	Article	IF	CITATIONS
145	Acid-Modified Natural Bauxite Mineral as a Cost-Effective and High-Efficient Catalyst Support for Slurry-Phase Hydrocracking of High-Temperature Coal Tar. Energy & Fuels, 2016, 30, 9203-9209.	2.5	15
146	MgAl-LDO mixed oxide derived from layered double hydroxide: A potential support for CoMo sulfur-resistant water–gas shift catalyst. Catalysis Communications, 2016, 78, 44-47.	1.6	15
147	Recent advances on nitrogen-doped metal-free materials for the selective catalytic oxidation of hydrogen sulfide. Current Opinion in Green and Sustainable Chemistry, 2020, 25, 100361.	3.2	15
148	Geometric and electronic modification of the active Fe3+ sites of α-Fe2O3 for highly efficient toluene combustion. Journal of Hazardous Materials, 2020, 398, 123233.	6.5	15
149	Engineering of Ce3+-O-Ni structures enriched with oxygen vacancies via Zr doping for effective generation of hydrogen from ammonia. Chemical Engineering Science, 2021, 245, 116818.	1.9	15
150	Improving conversion of methyl palmitate to diesel-like fuel through catalytic deoxygenation with B2O3-modified ZrO2. Fuel Processing Technology, 2022, 226, 107091.	3.7	15
151	Low-Temperature Desulfurization on Iron Oxide Hydroxides: Influence of Precipitation pH on Structure and Performance. Industrial & Engineering Chemistry Research, 2015, 54, 2419-2424.	1.8	14
152	Effect of Ce modification on the structural and catalytic property of Co-Mo/Mg(Al)O catalyst for water-gas shift reaction. Applied Catalysis A: General, 2018, 553, 36-42.	2.2	14
153	Preparation of a Highly Efficient Carbon-Supported Ruthenium Catalyst by Carbon Monoxide Treatment. Industrial & Engineering Chemistry Research, 2018, 57, 2819-2828.	1.8	14
154	Hybrid Mo–C <sub><i>T</i></sub> Nanowires as Highly Efficient Catalysts for Direct Dehydrogenation of Isobutane. ACS Applied Materials & Interfaces, 2018, 10, 23112-23121.	4.0	14
155	Zeolite-seed-directed Ru nanoparticles highly resistant against sintering for efficient nitrogen activation to ammonia. Science Bulletin, 2020, 65, 1085-1093.	4.3	14
156	Construction of a Pd(PdO)/Co <sub>3</sub> O <sub>4</sub> @SiO <sub>2</sub> core–shell structure for efficient low-temperature methane combustion. Nanoscale, 2021, 13, 5026-5032.	2.8	14
157	Slurry-Phase Hydrocracking of a Decalin–Phenanthrene Mixture by MoS <sub>2</sub> /SiO <sub>2</sub> –ZrO <sub>2</sub> Bifunctional Catalysts. Industrial & Engineering Chemistry Research, 2021, 60, 230-242.	1.8	14
158	Densities and viscosities of, and solubilities of acidic gases (SO2 and H2S) in natural deep eutectic solvents. Journal of Chemical Thermodynamics, 2022, 167, 106713.	1.0	14
159	Facile Synthesis and <scp>Highâ€Value</scp> Utilization of Ammonia. Chinese Journal of Chemistry, 2022, 40, 953-964.	2.6	14
160	Effects of A-site non-stoichiometry in YxInO3+δ on the catalytic performance during methane combustion. Physical Chemistry Chemical Physics, 2017, 19, 30418-30428.	1.3	13
161	Efficient low-temperature soot combustion by bimetallic Ag–Cu/SBA-15 catalysts. Journal of Environmental Sciences, 2018, 64, 122-129.	3.2	13
162	Cu incorporated perovskite Na0.5Bi0.5TiO3 oxygen-defect conductor as NO2 sensor using CuO sensitive electrode. Ceramics International, 2019, 45, 8494-8503.	2.3	13

#	Article	IF	CITATIONS
163	Unraveling the Role of Cu <sup>0</sup> and Cu <sup>+</sup> Sites in Cu/SiO <sub>2</sub> Catalysts for Waterâ€Gas Shift Reaction. ChemCatChem, 2020, 12, 4672-4679.	1.8	13
164	Hydrogen Production via Water–Gas Shift Reaction by Cu/SiO <sub>2</sub> Catalyst: A Case Study of CeO <sub>2</sub> Doping. Energy & Fuels, 2021, 35, 3521-3528.	2.5	13
165	Titanium modified Ru/CeO2 catalysts for ammonia synthesis. Chemical Engineering Science, 2022, 251, 117434.	1.9	13
166	Hydrogen production from ammonia decomposition over Ni/CeO2 catalyst: Effect of CeO2 morphology. Journal of Rare Earths, 2023, 41, 1014-1021.	2.5	13
167	Essential Role of Ru–Anion Interaction in Ru-Based Ammonia Synthesis Catalysts. ACS Catalysis, 2022, 12, 7633-7642.	5.5	13
168	From cheap natural bauxite to high-efficient slurry-phase hydrocracking catalyst for high temperature coal tar: A simple hydrothermal modification. Fuel Processing Technology, 2018, 175, 123-130.	3.7	12
169	Preparation of CuO/CeO <sub>2</sub> Catalyst with Enhanced Catalytic Performance for Water–Gas Shift Reaction in Hydrogen Production. Energy Technology, 2018, 6, 1096-1103.	1.8	12
170	Dual-template approach to designing nitrogen functionalized, hierarchical porous carbons for efficiently selective capture and separation of SO2. Separation and Purification Technology, 2022, 284, 120272.	3.9	12
171	Bimetallic Metal–Organic Frameworks MIL-53( <i>x</i> Al– <i>y</i> Fe) as Efficient Catalysts for H <sub>2</sub> S Selective Oxidation. Inorganic Chemistry, 2022, 61, 3774-3784.	1.9	12
172	Efficiently Integrated Desulfurization from Natural Gas over Zn-ZIF-Derived Hierarchical Lamellar Carbon Frameworks. Inorganic Chemistry, 2022, 61, 6083-6093.	1.9	12
173	Controlled preparation of Ni–Cu alloy catalyst via hydrotalcite-like precursor and its enhanced catalytic performance for methane decomposition. Fuel Processing Technology, 2022, 233, 107271.	3.7	12
174	Hydrogen production by water-gas shift reaction over Co-promoted MoS2/Al2O3 catalyst: The intrinsic activities of Co-promoted and unprompted sites. International Journal of Hydrogen Energy, 2018, 43, 7405-7410.	3.8	11
175	Geometric synergy of Steam/Carbon dioxide Co-electrolysis and methanation in a tubular solid oxide Electrolysis cell for direct Power-to-Methane. Energy Conversion and Management, 2020, 208, 112570.	4.4	11
176	N-Induced Electron Transfer Effect on Low-Temperature Activation of Nitrogen for Ammonia Synthesis over Co-Based Catalysts. ACS Sustainable Chemistry and Engineering, 2021, 9, 1529-1539.	3.2	11
177	Tuning N2 activation pathway over Ru/Co sub-nanometer alloy for efficient ammonia synthesis. Journal of Catalysis, 2021, 404, 440-450.	3.1	11
178	Studies of a Highly Active Cobalt Atomic Cluster Catalyst for Ammonia Synthesis. ACS Sustainable Chemistry and Engineering, 2022, 10, 1951-1960.	3.2	11
179	Molybdenum carbide phase effects in heterogeneous catalytic ammonia synthesis. Chemical Engineering Science, 2022, 259, 117834.	1.9	11
180	Controlling the synthesis and application of nanocrystalline spherical and ordered mesoporous alumina with high thermal stability. RSC Advances, 2015, 5, 93917-93925.	1.7	10

#	Article	IF	CITATIONS
181	Highly efficient Cu <sub>x</sub> O/TiO <sub>2</sub> catalysts: controllable dispersion and isolation of metal active species. Dalton Transactions, 2016, 45, 4491-4495.	1.6	10
182	Mg–Al hydrotalcite-supported Pd catalyst for low-temperature CO oxidation: effect of Pd <sup>n+</sup> species and surface hydroxyl groups. Dalton Transactions, 2018, 47, 14938-14944.	1.6	10
183	Construction and evolution of active palladium species on phase-regulated reducible TiO <sub>2</sub> for methane combustion. Catalysis Science and Technology, 2021, 11, 836-845.	2.1	10
184	Facile fabrication of hollow tubular mixed oxides for selective catalytic reduction of NOx at low temperature: a combined experimental and theoretical study. Chemical Communications, 2017, 53, 967-970.	2.2	9
185	Promoting Effects of Lanthan on Ru/AC for Ammonia Synthesis: Tuning Catalytic Efficiency and Stability Simultaneously. ChemistrySelect, 2017, 2, 6040-6046.	0.7	9
186	Synthesis, Characterization, and Catalytic Performance of Aminomethylphosphonic Molybdenum Catalysts for Slurry-Phase Hydrocracking. Industrial & Engineering Chemistry Research, 2019, 58, 2689-2696.	1.8	9
187	Ammonia-free synthesis of Mo/CoMgAl catalysts with excellent activities in water-gas shift reaction. Applied Catalysis A: General, 2019, 575, 58-64.	2.2	9
188	Effect of pore-size distribution on Ru/ZSM-5 catalyst for enhanced N2 activation to ammonia via dissociative mechanism. Journal of Rare Earths, 2020, 38, 873-882.	2.5	9
189	Influence of alloying on the catalytic performance of Ni–Al catalyst prepared from hydrotalcite-like compounds for methane decomposition. International Journal of Hydrogen Energy, 2021, 46, 3833-3846.	3.8	9
190	Porous flake-like Al-rich MgAl2O4 endowed with Mg vacancies for efficient oxidative desulfurization. Applied Catalysis A: General, 2021, 623, 118238.	2.2	9
191	Highly efficient subnanometer Ru-based catalyst for ammonia synthesis via an associative mechanism. Chinese Journal of Chemical Engineering, 2022, 43, 177-184.	1.7	9
192	Selective direct conversion of aqueous ethanol into butadiene <i>via</i> rational design of multifunctional catalysts. Catalysis Science and Technology, 2022, 12, 2210-2222.	2.1	9
193	Effects of cerium and tungsten addition on acid–base properties of spindle-like α-Fe2O3 in low-temperature SCR of NO with NH3. Journal of Rare Earths, 2022, 40, 1734-1742.	2.5	9
194	Enhanced catalytic performance of the carbon-supported Ru ammonia synthesis catalyst by an introduction of oxygen functional groups via gas-phase oxidation. Journal of Catalysis, 2022, 409, 78-86.	3.1	8
195	Carbon dioxide methanation over Ni catalysts prepared by reduction of Ni Mg3‒Al hydrotalcite-like compounds: Influence of Ni:Mg molar ratio. International Journal of Hydrogen Energy, 2022, 47, 22442-22453.	3.8	8
196	Defects modulating on MgAl-hydrotalcite nanosheet with improved performance in carbonyl sulfide elimination via a hydroxyl chemical looping route. Chemical Engineering Science, 2022, 259, 117827.	1.9	8
197	A Novel Highly Sensitive NO2 Sensor Based on Perovskite Na0.5+xBi0.5TiO3â^î^ Electrolyte. Scientific Reports, 2017, 7, 4997.	1.6	7
198	Target-oriented confinement of Ru-Co nanoparticles inside N-doped carbon spheres via a benzoic acid guided process for high-efficient low-temperature ammonia synthesis. Journal of Energy Chemistry, 2021, 57, 140-146.	7.1	7

#	Article	IF	CITATIONS
199	Boosting Efficient Ammonia Synthesis over Atomically Dispersed Co-Based Catalyst via the Modulation of Geometric and Electronic Structures. CCS Chemistry, 2022, 4, 1758-1769.	4.6	7
200	One-pot production of diethyl maleate <i>via</i> catalytic conversion of raw lignocellulosic biomass. Green Chemistry, 2021, 23, 10116-10122.	4.6	7
201	Sustainable synthesis of ordered mesoporous materials without additional solvents. Journal of Colloid and Interface Science, 2022, 619, 116-122.	5.0	7
202	Total oxidation of benzene over cobalt-aluminum mixed oxides prepared from layered double hydroxides: influence of preparation methods. Reaction Kinetics, Mechanisms and Catalysis, 2016, 118, 593-604.	0.8	6
203	Structural Evolution of Active Entities on Co <sub>3</sub> O <sub>4</sub> /CeO <sub>2</sub> Catalyst during Water Gas Shift Reaction. Industrial & Engineering Chemistry Research, 2019, 58, 17692-17698.	1.8	6
204	Investigation on Deactivation of Kâ€promoted Ru Catalyst for Ammonia Synthesis by CO Formation. ChemistrySelect, 2020, 5, 6639-6645.	0.7	6
205	Hydrotalcite-derived aluminum-doped cobalt oxides for catalytic benzene combustion: Effect of calcination atmosphere. Molecular Catalysis, 2022, 520, 112160.	1.0	6
206	Enhancement of ammonia synthesis activity on La2O3-supported Ru catalyst by addition of ceria. International Journal of Hydrogen Energy, 2022, 47, 23240-23248.	3.8	6
207	Electronic Regulation of Bromophenyl Grafted Metalâ€Free Carbon Nitride Catalysts for Enhanced Utilization of H <sub>2</sub> S. ChemCatChem, 2021, 13, 2386-2392.	1.8	5
208	A solid thermal and fast synthesis of MgAl-hydrotalcite nanosheets and their applications in the catalytic elimination of carbonyl sulfide and hydrogen sulfide. New Journal of Chemistry, 2021, 45, 3535-3545.	1.4	5
209	Ru alloying with La or Y for ammonia synthesis via integrated dissociative and associative mechanism with superior operational stability. Chemical Engineering Science, 2021, , 117255.	1.9	5
210	Metal 3D Printed Nickelâ€Based Self atalytic Reactor for COx Methanation. ChemCatChem, 2022, 14, .	1.8	5
211	Tuning defect nonequilibrium of brownmillerite Sr1+xY2-xO4+Î′ for rich-oxygen-vacancy direct ammonia solid oxide fuel cells cathode. Journal of Power Sources, 2022, 524, 231078.	4.0	4
212	Enhanced ammonia synthesis activity of carbon-supported Mo catalyst by Mo carburization. Chemical Communications, 2022, 58, 7785-7788.	2.2	4
213	Enabling High Efficiency and Rapid Regeneration of α-FeOOH@Fe-EDTA for Slurry Desulfurization. Industrial & Engineering Chemistry Research, 2022, 61, 249-258.	1.8	3
214	Three-dimensional ordered macroporous Ru-substituted BaZrO <sub>3</sub> perovskites: active catalysts for ammonia synthesis under mild conditions. Catalysis Science and Technology, 2019, 9, 6217-6221.	2.1	2
215	Exploring N-Containing Compound Catalyst for H2S Selective Oxidation: Case Study of TaON and Ta3N5. Catalysis Letters, 2021, 151, 1728-1737.	1.4	2
216	Zirconia prepared from UIO-66 as a support of Ru catalyst for ammonia synthesis. Chinese Chemical Letters, 2023, 34, 107237.	4.8	2

#	Article	IF	CITATIONS
217	AÂNew Catalyst Support Made of Bauxite: Preparation and Catalytic Properties. Zeitschrift Fur Physikalische Chemie, 2014, 228, 49-62.	1.4	1
218	Direct ammonia solid oxide fuel cells based on spinel ACo2O4 (A=Zn, Fe, Ni) composite cathodes at intermediate temperature. International Journal of Green Energy, 0, , 1-10.	2.1	1